J. R. Villemonte, J. A. Hoopes,
D. S. Wu and T. M. Lillesand

REMOTE SENSING IN THE MIXING ZONE

REMOTE SENSING IN THE MIXING ZONE

J. R. Villemonte, J. A. Hoopes,
D. S. Wu and T. M. Lillesand

Department of Civil and Environmental Engineering
University of Wisconsin—Madison

Institute for Environmental Studies
Remote Sensing Program

Report No. 22

August 1973

*

1

I. INTRODUCTION

Background. The genealogy of the work reported in this paper stems from a mixing zone research project originated in 1968 and supported financially by the Department of Natural Resources of the State of Wisconsin. The central objective was the study of the characteristics of dispersion and diffusion as the mechanisms by which pollutants are transported in natural river courses, with the view of providing additional data for the establishment of water quality guidelines and effluent outfall design protocols.

The first year involved a comprehensive study of the literature and some laboratory model observations from which there developed a compendium of reference materials, some qualitative conclusions regarding the effects of certain outfall, effluent and river characteristics on mixing rates, and a functional hypothesis for the extent of the mixing zone in terms of these characteristics. The second year included the first field surveys (during the summer of 1969) together with the beginnings of laboratory model studies of one of the field sites. At this time also the mixing zone project became part of a larger interdisciplinary Remote Sensing Program administered by the University's Institute for Environmental Studies and financed by the Office of University Affairs of the National Aeronautics and Space Administration (NASA). This evolvement was natural, because the summer field surveys of 1969 brought out the inadequacy of ground activities alone for covering large geographic areas, namely that observed data are largely either static or time averaged. Over the last three years additional ground and aerial field surveys and laboratory modelling have been undertaken. In addition, mathematical modelling and quantitative photographic delineation of the mixing zone have been initiated.

Project Goals. Throughout this investigation, work has been divided into four basic categories which are directed at the basic goal of developing relationships which will permit the estimation of the nature and extent of the mixing zone as a function of those variables which characterize the outfall structure, the effluent, and the river, as well as climatological conditions. These relationships may be used (a) in the establishment of definite and rational water quality guidelines, (b) in the development of a sampling and surveillance program by governmental and private agencies, and (c) in the development of a protocol for the design and location of waste effluent outfalls.

The four basic categories of effort are:

1. The development of mathematical models.

2. Laboratory studies of physical models.

3. Field surveys involving ground and aerial sensing.

4. Correlation between aerial photographic imagery and mixing
    zone characteristics.

In category (1) simple jet- and source-type, two- and three-
dimensional mathematical models have been constructed and compared
with field observations. Detailed mathematical modelling, including
more realistic approximations of the flow field and river and
outfall geometry, is being undertaken. The work in Category (2)
has led to observations and measurements of temperature patterns
in laboratory models of the Weston power plant (see site descrip-
tions) and to considerations of scaling in such models. The work
in Category (3) includes field measurements of effluent discharge
mixing patterns at seven sites throughout the State. These surveys,
which have been carried out over the past four years, will be con-
tinued with intensive ground-aerial measurements at one site. In
Category (4), a method has been developed which relates aerial
photographic film response (film density) to surficial suspended
solids concentrations in the paper mill discharge at the Kimberly-
Clark plant and the sewage treatment plant (STP) discharge at
Neenah-Menasha (see site descriptions). The work in this category
will be intensified and move in somewhat different directions as a
result of the work done thus far.

Scope of this Report. The general objective of this report is to
give an overview of the project goals and activities to date,
together with a conceptual discussion of the mixing zone definition
and measurements associated therewith. Accordingly it will be
necessary to show the powerfully good consequences of coordinating
ground and aerial techniques and methods, in contrast to their
inadequacies when separated. In addition, sufficient results will
be presented to serve as indicators of the type of work accomplished
and yet to evolve as the work proceeds. Three of the seven field
sites will be used in order to cover a fairly wide spectrum of waste
effluent situations indigenous to the industries and municipalities
of the State of Wisconsin (see site descriptions).

II. DEFINITION OF THE MIXING ZONE

Whenever two or more fluid substances are brought together, a
mixing zone or region is created within the regime of flow. The
characteristics of the mixing zone are related to the convective
transport mechanisms of diffusion and dispersion. The transport
associated with diffusion can be due either to molecular or turbulent
actions. In most real life situations the "time" is so short that
the action of molecular diffusion can be neglected. Therefore, in
the mixing zone, diffusion is only the result of turbulent action.

If the fluids which come together are composed of identical substances, the characteristics of the mixing zone can be measured only by the momentum and energy distribution coefficients and the turbulent energy spectra. Manifestations of these are the velocity and energy gradients throughout the regime. Two homely examples of this situation are the confluence of rivers and the impingement of the air from a ventilating duct outlet into the air of a room, where the compositions of the fluids, in both examples, are the same.

If the fluids which come together are not composed of identical substances, then the characteristics of the mixing zone can be more completely defined by the additional measurement of the distribution of the concentration of one of the substances within the other. The most common examples of this situation involve the introduction of effluent wastes into lakes, rivers and streams. The effluent wastes from domestic sewage treatment plants, industrial plant operations, and from thermal power generating plants are the most common in relation to their impacts on the earth's environment.

Since the mixing zones of the second case can be measured more completely utilizing changes in concentration, it is practical to convert Case 1 into Case 2 through the introduction of tracer elements, which can be either chemical or particulate in nature. Thus it is possible to use fluorescent dyes and nuclear isotopes in such minute quantities that they do not affect the diffusion and dispersion transport characteristics, but their concentrations can be measured easily with adequate accuracy.

The physical mixing zone region is defined as that portion of the flow regime in which the tracer (or effluent waste) is diluted to the concentration obtainable by total or complete mixing at the point of discharge. Such a definition presupposes that the flow regime and the tracer regime have the initial properties of real fluids in motion (at least mass density and absolute viscosity) and are subjected to the constraints of real physical boundaries.

The dilution processes are related to the convective transport mechanisms of diffusion and dispersion, as mentioned earlier. This mixing activity is accomplished in two stages, each having its own logical part of the mixing zone region.

Stage one is always the first part of the zone. Here the exchange of momenta is on a macro-scale, since the initial conditions of velocity, linear momentum, turbulence levels, and turbulent energy spectra of the flow regime and effluent wastes are not the same (if they were, stage one would not exist). Thus, the mixing and dilution processes are largely dispersive in nature, because the scattering is clearly visible and is manifest by macroscopic eddies and swirls clearly different in character than those of the ambient regime.

Stage two begins at the completion of the macro-scale activity, therefore the velocity, momentum, and turbulence characteristics of the zone and the ambient regime are about the same. They can't be exactly the same, however, since the two liquids ordinarily have different suspended solids, temperatures, and kinematic viscosities, each of which has an effect on the turbulence level for a given energy gradient. It naturally follows that the dilution process in stage two is on a relatively small scale and is the result largely of turbulent diffusion.

Stage two of the zone ends when all of the characteristics of the zone and the ambient are the same, or as stated previously, when the tracer is diluted to the concentration obtainable by complete mixing. It can also be said that stage two cannot be seen by the human eye, unless of course the effluent waste has visible characteristics different from those of the ambient regime.

III. MEASURING THE MIXING ZONE

The fluid dynamic, thermal, and water quality characteristics of the mixing zone can be quantified using both ground and aerial sensing methods in complimentary ways. By so doing it is important to realize the separate and coordinate roles which each plays.

The ground measurements, although slow and tedious, define the vertical variations and provide the data for correlating aerial photographic imagery and effluent wastes concentrations. The aerial sensing methods relate to the collapse of the time scale. In a matter of a few minutes the surficial layer several miles long and wide can be photographed. In a sense the aerial measurements "stop the clock" and thus show the extensiveness of the zone, its transient nature, as well as provide relative film densities. This is an excellent example of the benefits that can be derived when several disciplines are brought together in such a way as to maximize the results.

In the presentation of results more detailed descriptions of the ground and aerial sensing techniques and methods of analysis are given.

IV. DESCRIPTION OF FIELD SITES

The Weston Power Plant. The plant is a 135 megawatt steam electric, fossil-fueled, unit located on a fairly straight reach of the Wisconsin River a few miles south of Wausau near Rothschild. The

plant is 40 percent efficient and takes in condenser cooling water from the river through an intake of traditional design, except that the water passes over drum screens to remove the suspended solids introduced by paper mill operations upstream near Wausau. The screenings are continuously flushed off the drum and reintroduced into the river in the locale of the effluent outfall, as shown in figure 1.

The warm water effluent is discharged through a reinforced concrete structure, whose opening is 6 ft by 8 ft and submerged about 3 ft, into a small bay. The bay is connected to the river by a canal whose centerline is pointing about 45 degrees downstream from a normal to the river flow pattern.

The river width is about 500 ft, and under average conditions, the depth is about 5 ft, thereby producing a width to depth ratio of 100. The normal summer discharge of the river is 2000 cfs, with a velocity of about 1.0 fps. The discharge and velocity ratios (river to effluent) were 10 and 0.25, respectively.

The Waukesha Sewage Treatment Plant. The municipal sewage from the City of Waukesha, Wisconsin, is handled in a plant having secondary treatment and located on the Illinois Fox River just south of the city. The effluent is discharged into the river on the left bank through a 30-in. diameter culvert pipe aligned about 30 degrees to the axis of the river. In this region the river is very winding, and the outfall is located at the end of a large double bend, as is shown in figure 2.

The river width is 80 ft on the average with a depth of 1.0 ft, so that the width to depth ratio is   80. The normal summer river discharge is about 40 cfs, with a velocity of 0.7 fps. The discharge and velocity ratios (river to effluent) were 2.6 and 0.25, respectively.

The Kimberly-Clark Paper Mill. The mill is located at the Cedars Dam on the Lower Fox River near Kimberly, Wisconsin. The plant manufactures special types of paper for color printing (photographic magazines, etc.) and discharges about 50,000 lbs per day of effluent wastes contining dyes, kaolins, titanium dioxide, pulp, etc.

The mill has a total of 25 outfalls, four of which are located on the upstream side of Cedars Dam, and the remainder on the downstream side. The discharges from the downstream outfalls combine into one plume along the south bank of the river, as shown in figure 3. About 65 percent of this discharge comes from the main mill outfall which is a U-shaped channel having an area of about 3.2 sq ft.

The river downstream from Cedars Dam bends to the right and widens from 600 ft to 1000 ft beyond the exit channel from the dam
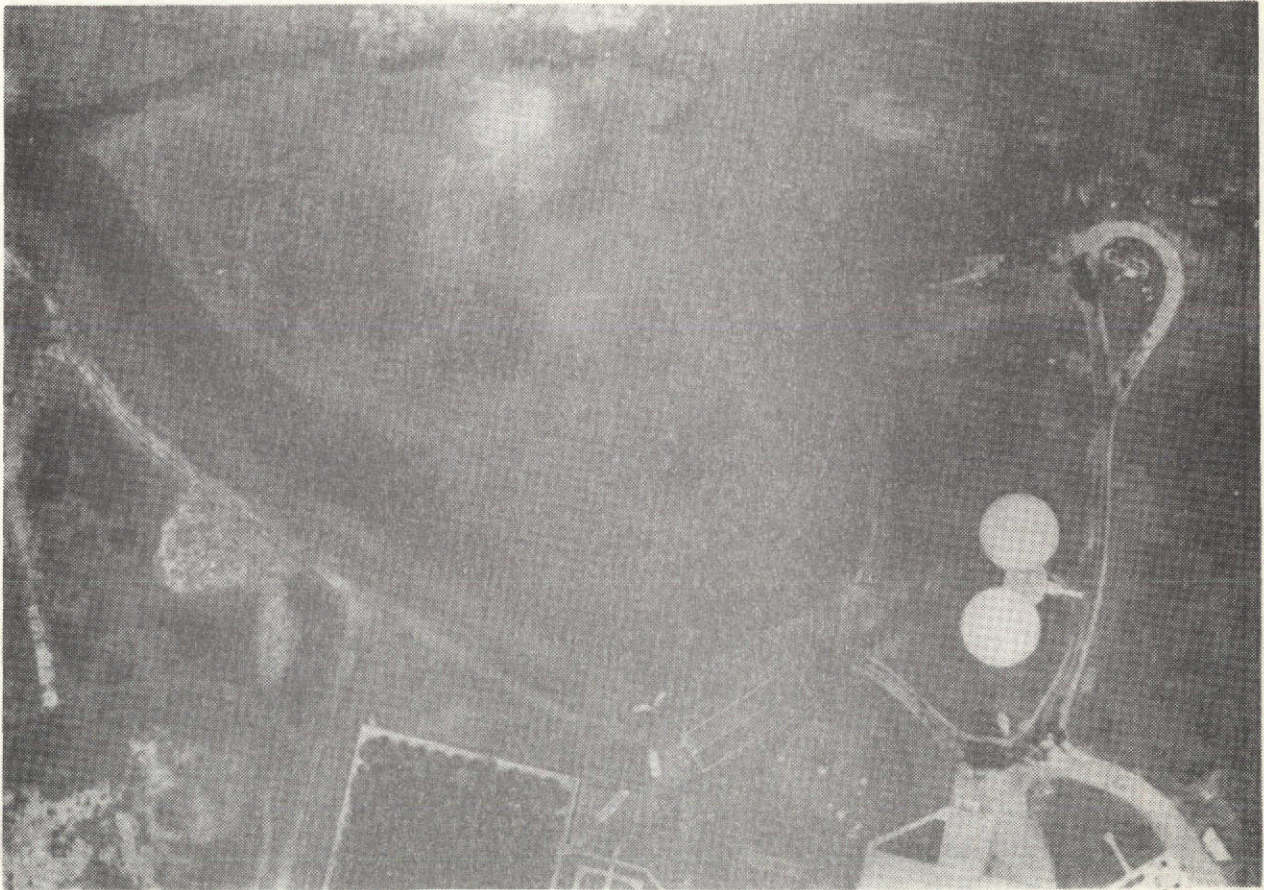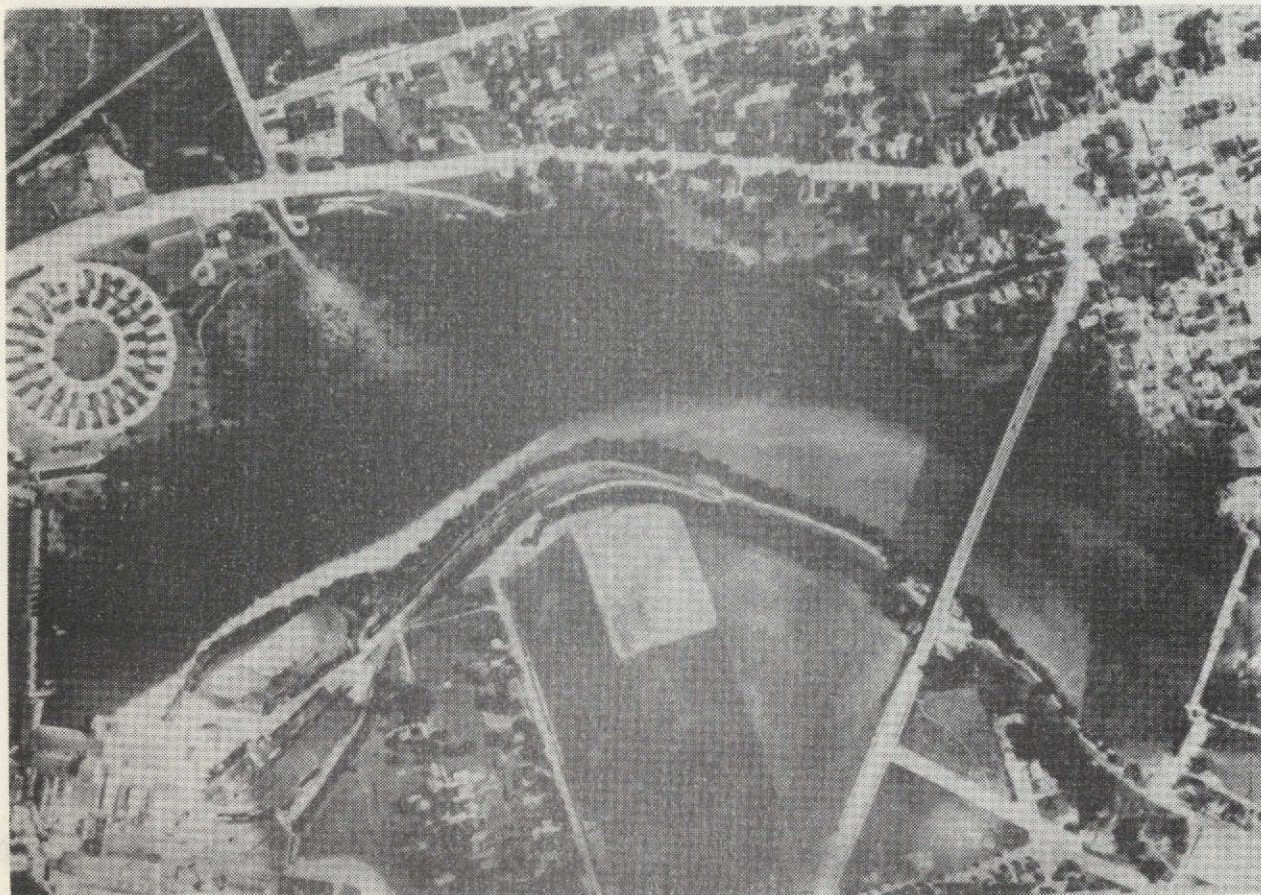
Figure 1. Aerial Photo of Weston Power Plant Site.
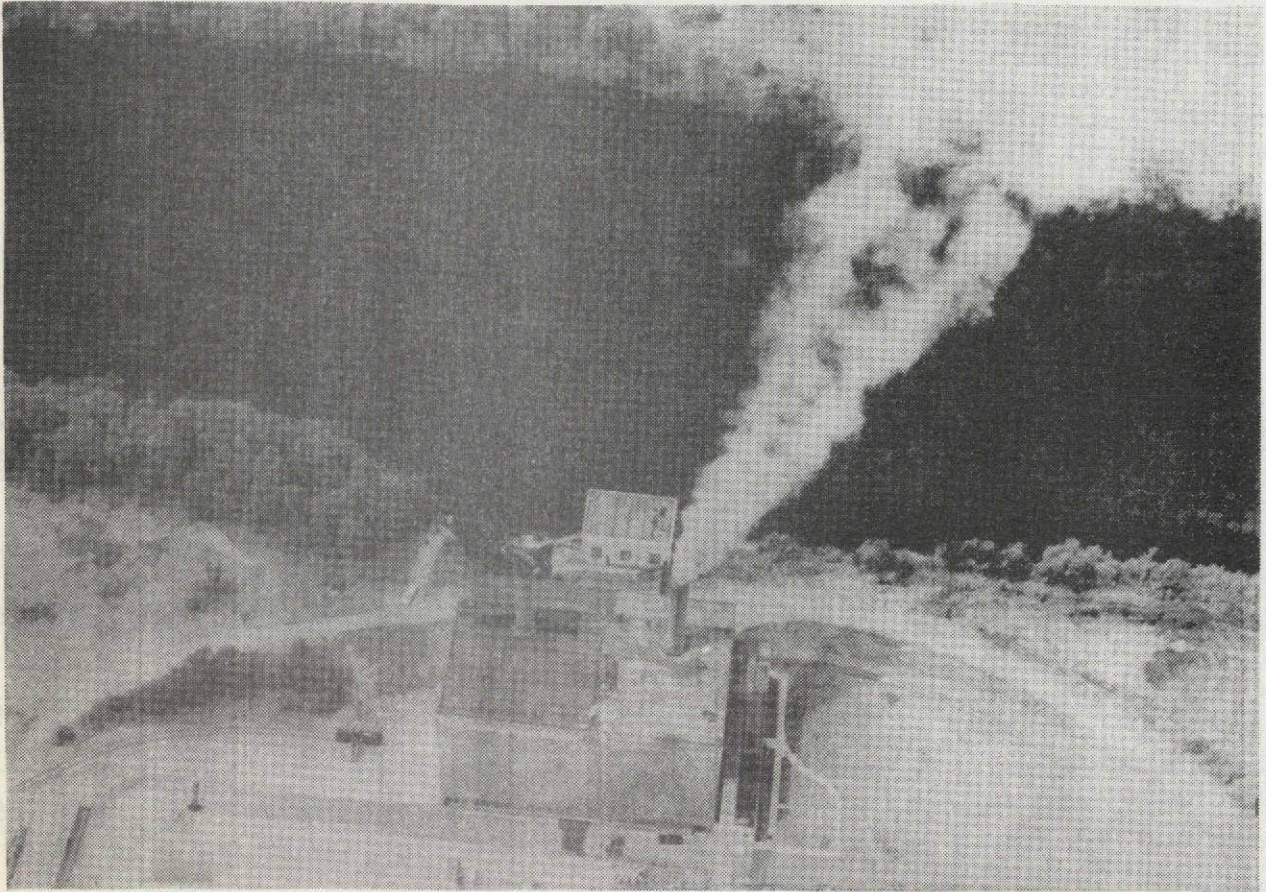
This page is reproduced at the back of the report by a different reproduction method to provide better detail.

Figure 2. Aerial Photo of Waukesha Sewage Treatment Plant Site.

Figure 3. Aerial Photo of Kimberly-Clark Paper Mill Site.

locks. About 0.75 miles downstream from the Cedars Dam is Little
Chute Dam, which fact produces a mixing zone that enters the upstream
or delta region of an impoundment. The river depth varies from
5 to 10 ft.

The normal summer river discharge is 1700 cfs with a velocity
which is somewhat greater than 1.0 fps at the dam and less than 0.3
fps upstream from the Little Chute Dam. The discharge and velocity
ratios (river to effluent) were 120 and 0.20, respectively.

V. PHOTOGRAPHIC AND THERMAL IMAGERY

Background. Ground measurements at each of the sites were initially
supported by 35 mm color and color infrared photography obtained
during exploratory aerial measurements taken in developing an inven-
tory of pollution sites throughout the State. In most cases the
photographs depicted in a rather vivid but qualitative way the
presence, extent, and character of the mixing zone.

Microdensitometric analysis of the photography of the Neenah-
Menasha STP outfall suggested a very probable correlation between
image densities and the level of concentration of suspended solids
in the surficial layer (top 0.5 ft) of the mixing zone. It was
decided to pursue the validity of the correlation by accelerated
and more intensive measurements at the Kimberly-Clark Paper Mill
site.

In addition, aerial thermal scanning also has been utilized at
several sites to extend and complement ground measurements of
temperature patterns. The application and results of this method
for the Kimberly-Clark Mill site are presented herein.

Photographic Image Density Model Development. Laboratory reflectance
analyses performed by Scherz and Klooster(4) were used to demonstrate
that water sample reflectance is a function of turbidity and the
related suspended solids found in samples taken from the Kimberly-
Clark mixing zone and ambient regions. From these data it can be
shown that for a given wavelength and for solids concentrations
less than about 200 mg/l, the relationship takes the form,

$$R = K_1 S + K_2 \quad - - - - - - - - - - - - - - (1)$$

where R is the water sample reflectance, S is the concentration of
suspended solids in mg/l, and K_1 and K_2 are parameters.

The film exposure can be related to scene reflectance by the
expression,

$$E = K_3 R + K_4 \quad - - - - - - - - - - - - - - (2)$$

where $\underline{E}$ is the exposure of the film, $\underline{R}$ is the scene reflectance, and $\underline{K_3}$ and $\underline{K_4}$ are also parameters.

The image optical density resulting from relative film exposure can be determined on the basis of a film-step wedge calibration. The resulting functional expression, as shown by Dana(2), can take the form,

$$D = B_o + B_1 Z + B_2 Z^2 + B_3 Z^3 \text{ } - - - - - - - \quad (3)$$

where $\underline{D}$ is the image optical density; $\underline{B_o}$, $\underline{B_1}$, $\underline{B_2}$, and $\underline{B_3}$ are film type, handling, and processing parameters; and $\underline{Z}$ is equal to relative Log E.

Equations (1) through (3) permit the development of an expression (model) which permits the estimation of suspended solids, $\underline{S}$, from the measurable image density, $\underline{D}$, so that,

$$S = \alpha 10^{Z(D)} + \beta \text{ } - - - - - - - - - - - - - \quad (4)$$

where $\underline{\alpha}$ and $\underline{\beta}$ are model parameters and $\underline{Z}(D)$ results from the solution of equation (3).

Application of Image Density Model. The model manifested by equation (4) was used in the study of the Kimberly-Clark Paper Mill mixing zone. The image optical densities were extracted from each of the three layers (red, green, and blue) of color infrared film type 8443. Concurrent with the aerial photography, suspended solids water samples were taken in the surficial layer at 82 locations. A photogrammetric solution for the image position associated with each sample location provided a viable means for obtaining simultaneous image densities and solids concentration.

The image densities were digitally recorded using a scanning microdensitometer system, which permitted discrete density observations over film areas depicting about 1.33 ft square areas on the ground. Experience showed that the image densities could be grouped into 36 density levels to give satisfactorily refined density observation (about 0.08 density units).

Equation (3) was solved for each observed density for corresponding values of $\underline{Z}$. The $\underline{B}$ parameters were estimated from the D versus $\underline{logE}$ curves resulting from the film calibration work. The suspended solids data resulting from the samples taken at the 82 locations were then used with these Z values to determine the α and β parameters. In both instances above, the curve fitting was done by least squares methods.

Figure 4 is a plot of the observed suspended solids and film density data. Also shown are the model predictions using a solution of equation (4). It is believed that the scatter of the data is due
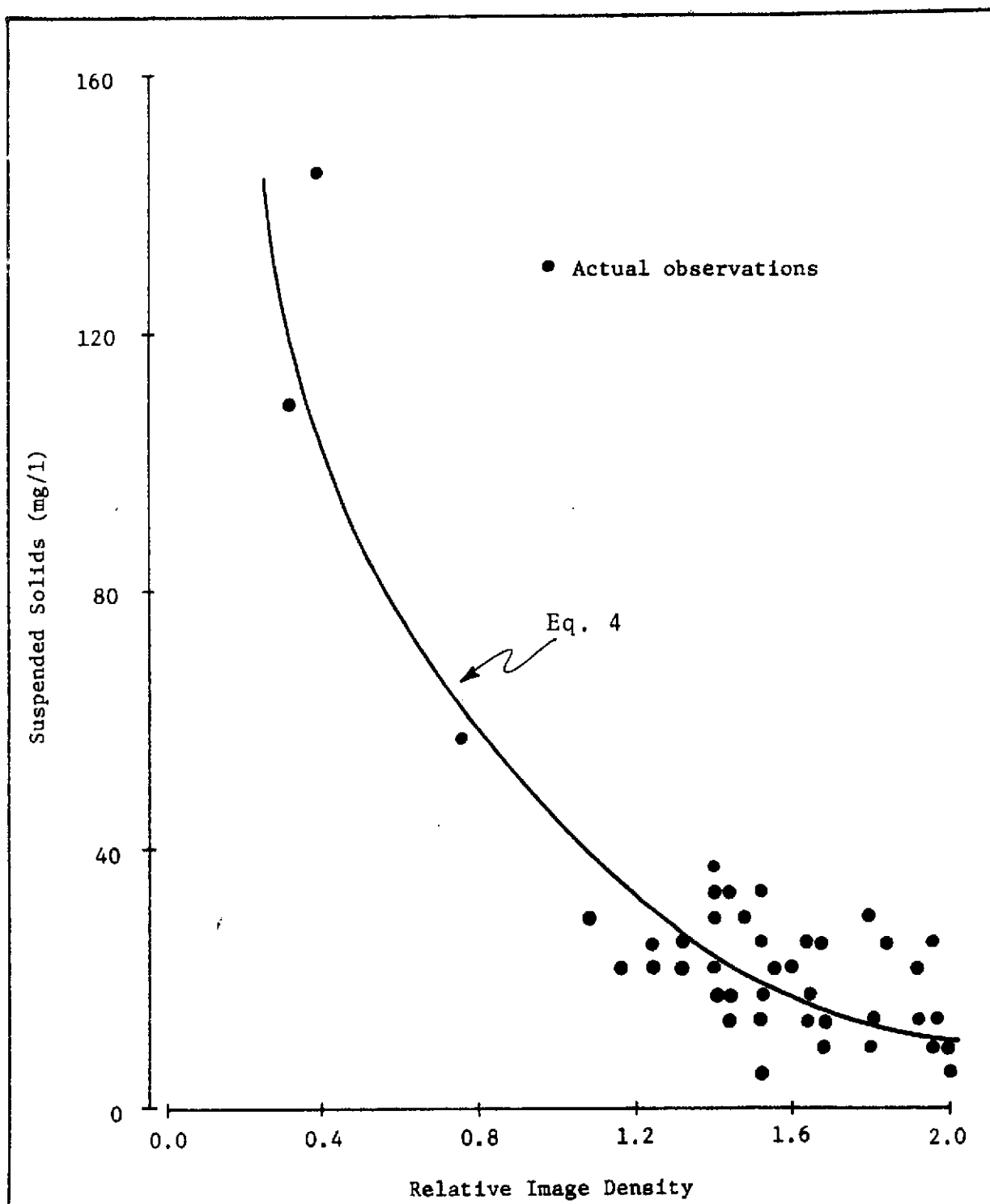
Fig. 4. Observed suspended solids versus relative image density for the Kimberly-Clark Paper Mill mixing zone.

largely to the experimental errors in obtaining and analyzing the water samples.

The model (equation (4) or figure 4) can be used with confidence for this particular mixing zone, provided the α and β parameters are determined for each roll of film. The applicability of this method to other types of suspended solids and mixing zones is a continuing objective of this program.

Application of Thermal Scanning. Infrared thermal imagery obtained from thermal scanners can be converted to surface water temperatures using the relation

$$H_{br} = A + BT + CT^2 - - - - - - - - - - - - (5)$$

where H_{br} = scanner output (proportional to emitted radiation), T = water surface temperature and A, B, C are parameters. Equation 5 is a close approximation to the integral of Planck's law for radiation over the 8-14 micron wave length range with corrections for the filter, gain and offset of the scanner. To utilize equation 5 and the 70 mm film output of the thermal scanner to determine water surface temperatures, the scanner film is first rectilinearized to correct for scanner distortions and enhanced to emphasize water temperatures and their variations relative to the land. Film density variations throughout the mixing zone are then determined using a microdensitometer and converted to a coded 256 level array (covering the maximum to minimum density variations) and stored on magnetic tape. Utilizing the known film density and water temperature at several positions throughout the mixing zone, the parameters A, B, and C in equation 5 can be evaluated. Subsequently, water temperatures can be determined for all other points where the film densities are known.

Figure 5 shows the surface temperature patterns, obtained from thermal imagery, for the Kimberly-Clark paper mill discharge into the Fox River at 1:00 PM on September 16, 1971. Similar results have been obtained at other sites and are being used to extend the ground measurements to cover the whole mixing zone.

VI.   MIXING PATTERNS

The ground and aerial observations at each of the sites provided the basic measurements for defining effluent concentration distributions and mixing patterns. Measurements of velocity, temperature and dye concentration and the taking of water samples at various locations throughout the mixing zone, along with plant and local climatic conditions, constituted the ground observations. Velocities were measured with Gurley, cup-type current meters having
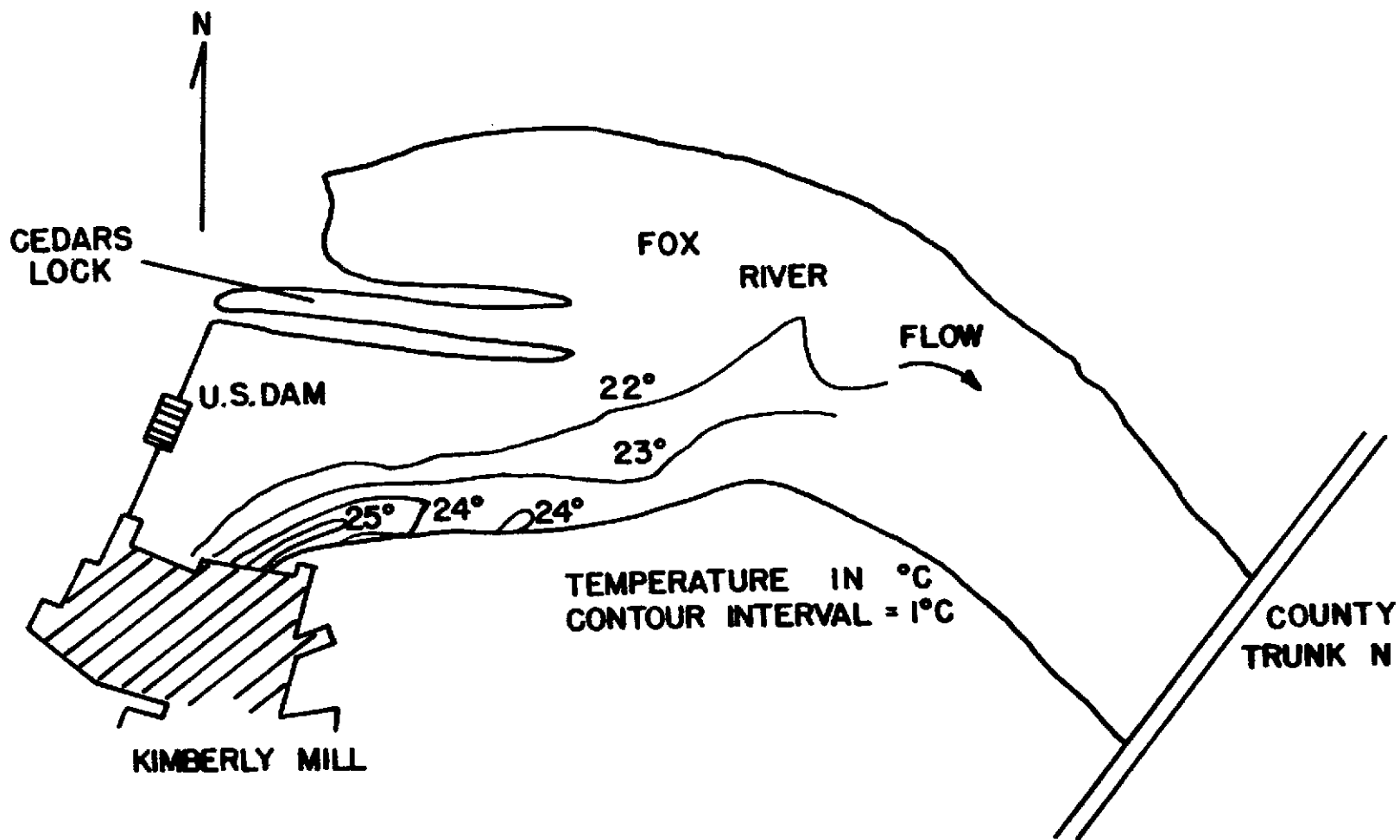
Figure 5. Surface temperature contours from thermal imagery at the Kimberly-Clark Paper Mill mixing zone. September 16, 1971.

both pulse and direct reading outputs. These meters were accurate to $\pm$ 0.1 fps. Temperatures were measured with a Whitney underwater thermometer having an accuracy of $\pm$ 0.1°C. Rhodamine WT dye, utilized at some sites as a tracer of effluent mixing patterns, was added to the effluent discharge and sensed at various points with a flow-through type Turner fluorometer. Water samples of 200 ml for suspended solids determination were taken with a specially built, multiple sampling device. Suspended solids were obtained by standard filtering and gravimetric methods. Each of these sensing devices was mounted in a 14 ft Jon boat used in the ground sampling program and was moved vertically over the river depth at each sampling station. These stations were generally located on sections perpendicular to the axis of the effluent discharge. The boat location was determined by the intersection of two, angular transit sightings from known positions along the shoreline.

To delineate concentration distributions and mixing patterns, the field data are plotted on horizontal and vertical cross sections and velocity and concentration contours are drawn. Analysis of these plots enables the determination of the rates of effluent spread and dilution, namely the variation of effluent width, flow rate, maximum concentration and trajectory and of turbulent diffusion coefficients with distance from the outfall. In the paragraphs below, two of these mixing characteristics (variation of effluent width and flow rate with distance from the outfall) are presented and discussed for several effluent, river and climatological conditions at the three field sites described earlier.

Weston Power Plant. Table I summarizes the effluent and river characteristics for five surveys. Figures 6 and 7 show the surface temperature distributions on two of the surveys.

The effluent temperature and velocity distributions reveal the two stages of mixing described previously in Section II. Near the plant (principally within the bay into which the outfall discharges) jet-induced mixing dominates the effluent dilution. Beyond 200 to 300 ft from the outfall, the effects of channel shape, turbulent diffusion and density differences (between effluent and river) control the spreading and dilution of the effluent. Figures 8 and 9 show the variation of effluent surface width, b, and flow rate, Q, with distance from the outfall for the two surveys in figures 6 and 7. These two characteristics clearly show the effects of changes in river, effluent and climatic conditions on effluent spreading and dilution, namely that decreases in Q_o/Q_r and increases in wind reduce the rate of lateral mixing. These effects can also be seen in figures 6 and 7. The surface width of the effluent, as determined by the color change between the effluent and river from 35 mm color aerial photographs, is in good agreement with the boat measurements, except for the July 15, 1970, survey when strong winds, and thus increased vertical mixing, made identification of the boundary from color change difficult.

Table I. Characteristics at Weston Power Plant for Field Surveys

Date	Q_o, cfs	Q_r, cfs	d, ft	W, ft	ΔT_o, °C	Q_o/Q_r	V_o/V_r	L_{mz}, ft x 10^{-3}	Climate
7/26/69	187	1800	4.87	533	10.6	0.10	3.7	17.4	10.7 mph wind, 25° air, cloudy
8/2/69	187	1600	4.01	518	9.9	0.12	4.7	14.1	8.3 mph wind, 25°C air, sunny
7/15/70	187	2750	3.71	514	11.3	0.07	2.4	54.0	14.0 mph wind, 22°C air, cloudy
8/26/70	187	1800	4.07	503	11.9	0.10	3.6	19.6	5.2 mph wind, 28°C air, sunny
7/22/71	187	2950	5.04	465	12.9	0.06	4.1	47.1	12.4 mph wind, 25°C air, cloudy

LEGEND

△ GROUND CONTROL STATION
— ISOTHERMS
∾ MIXING ZONE FRINGE
−− THERMAL EFFLUENT BOUNDARY
   DETERMINED FROM AERIAL PHOTOS

WESTON
POWER PLANT

SUBMERGED
OUTFALL

FILTER
WASH

34
33
32
31
30
29
28
27

FLOW
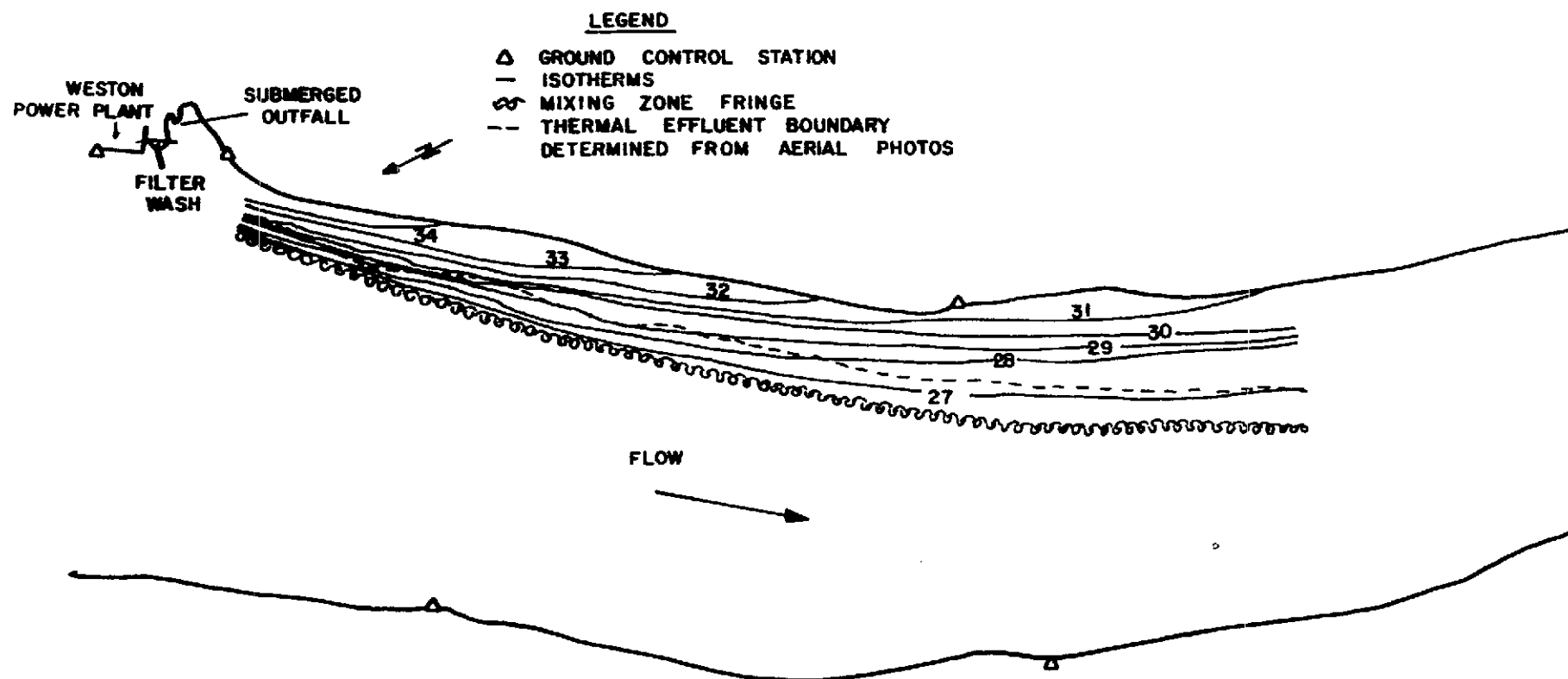
Figure 6. Surface temperature contours for the Weston Power Plant on July 15, 1970.

LEGEND

△ GROUND CONTROL STATION
▢ AERIAL TARGET
○ RANGE POLE
— ISOTHERMS
〜 MIXING ZONE FRINGE
--- THERMAL EFFLUENT BOUNDARY
DETERMINED FROM AERIAL PHOTOS

WESTON POWER PLANT

SUBMERGED OUTFALL

FILTER WASH

FLOW
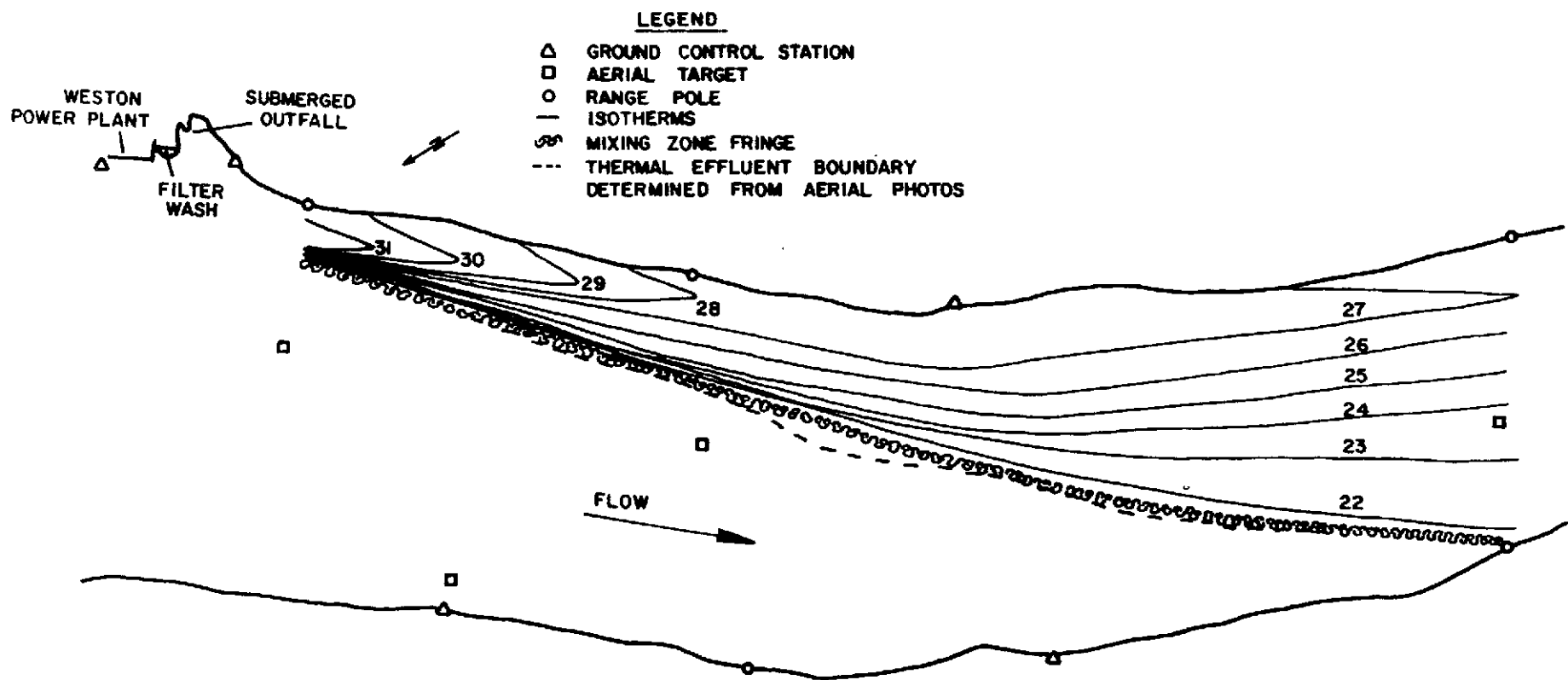
Figure 7. Surface temperature contours for the Weston Power Plant on August 26, 1970.
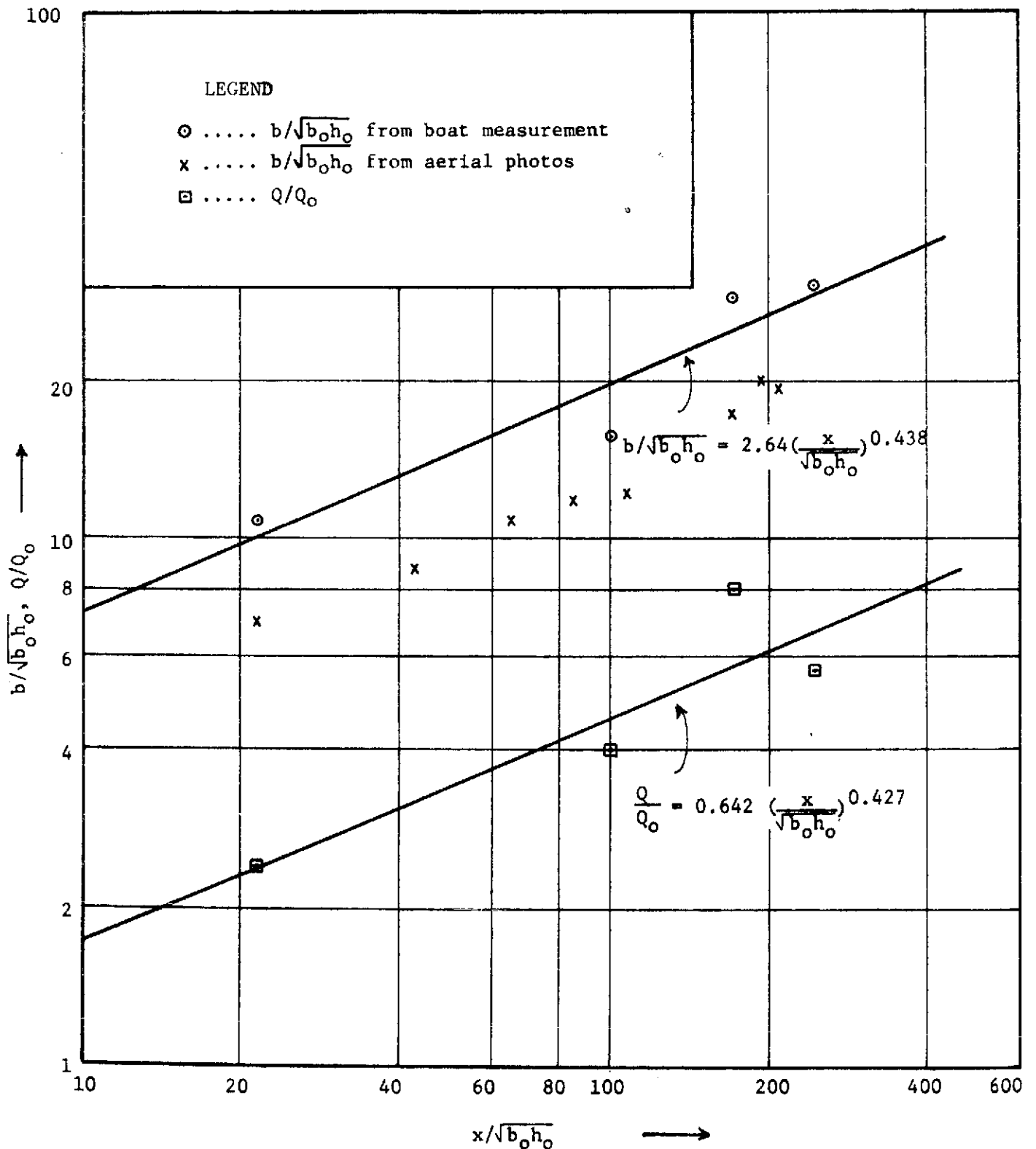
Fig. 8. Normalized distance from outfall versus mixing zone width and discharge for July 15, 1970, at Weston Power Plant.
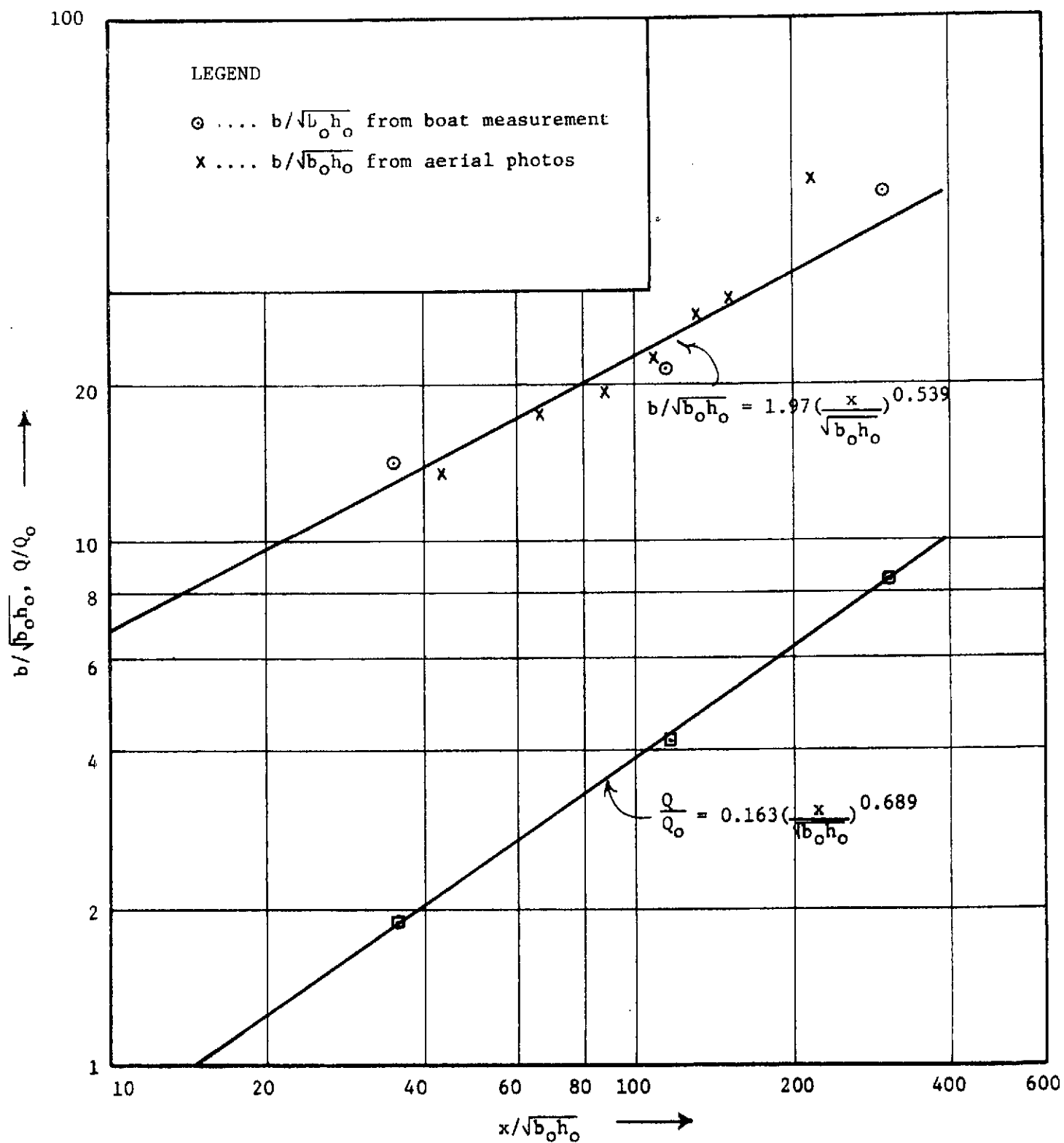
Fig. 9. Normalized distance from outfall versus mixing zone width and discharge for August 26, 1970, at the Weston Power Plant.

The vertical temperature distributions showed intense vertical mixing (vertical isotherms) on some surveys and pronounced tilting of isotherms on others. The vertical distributions are very sensitive to the intensity of the wind and secondarily to Q_o/Q_r and ΔT_o. For weak winds of less than 5-7 mph, vertical turbulent mixing was suppressed by density differences due to temperature, which resulted in increased lateral spreading and inclined isotherms. For strong winds of greater than 10-12 mph, vertical turbulent mixing generated vertical isotherms and a slower rate of lateral spreading. These effects can also be seen on figures 6 and 7.

Estimated lengths of the mixing zone for each survey, obtained from a two-dimensional, steady-state model of the temperature distribution (including surface heat loss and channel boundaries), are shown in Table I. These results show that the mixing zone length varies from 3 to 11 miles along the river and depends upon Q_o/Q_r and wind speed, in addition to the river velocity and depth and lateral diffusion coefficient. In accordance with the definition of the mixing zone, presented earlier, the temperature on the mixing zone boundary is given by $\Delta T_o(Q_o/Q_r)$. Extrapolation of the measured maximum surface temperature to this value indicates that the predicted mixing zone lengths in Table I are one order of magnitude too short. This significant discrepancy may result from the limited extent of the measurements, the three-dimensional nature of the actual temperature distribution, bends or other changes in channel geometry, and/or to errors in estimating the model parameters (diffusion coefficients, channel geometry and surface heat losses).

Waukesha STP. Table II summarizes river and effluent characteristics for five surveys. Figures 10 and 11 show the effluent concentration distribution for two surveys, as determined from temperature measurements.

As the river is shallow, the effluent mixes uniformly over the depth due to turbulence generated by bottom frictional resistance and wind shear. Meteorological conditions, in general, appear to have little effect on currents or spreading patterns. Up to 30 to 50 ft downstream of the outfall, the effluent spreads rapidly across the river (due to the initial momentum of the discharge relative to the river and the angle of discharge) to a width, b_o, which increases linearly with Q_o/Q_r. Beyond this initial region, and over the region of measurements, the effluent spread is controlled by lateral turbulent mixing (and to some extent, channel geometry) such that
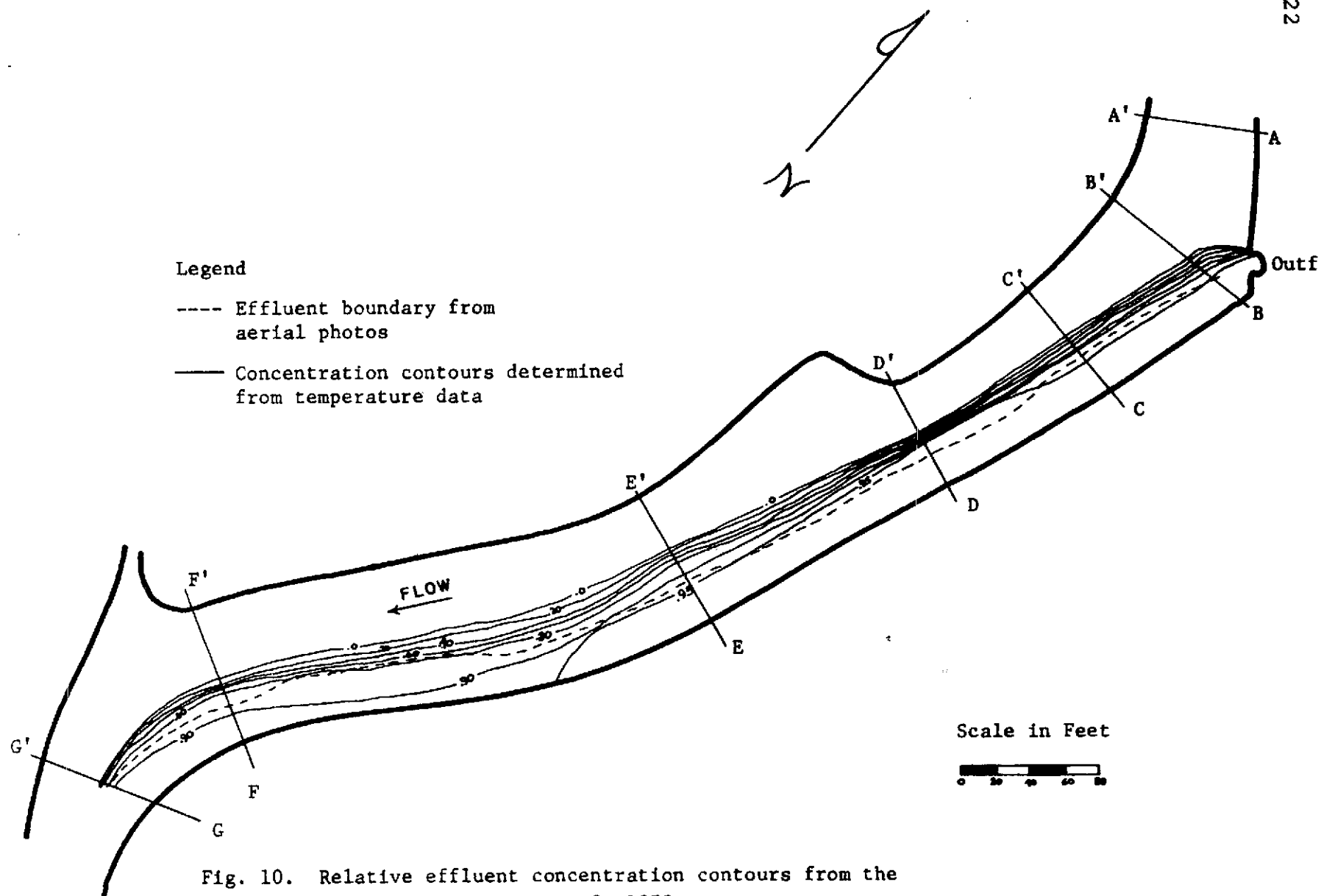
$$b = b_o + \sqrt{2D_y\,x/V_r} \quad - - - - - - - - - - - \quad (6)$$

where b is effluent width, D_y is lateral turbulent diffusion coefficient, x is distance from outfall and V_r is river velocity. As

Table II. Characteristics at Waukesha STP for Field Surveys

Date	Q_o, cfs	Q_r, cfs	d, ft	W, ft	Q_o/Q_r	b_o/W	V_o/V_r	L_{mz}, ft	Climate
8/9/69	14.7	62.1	0.77	87	0.24	0.30	3.2	1.6×10^5	10 mph wind, 20°C air, drizzle
8/16/69	14.1	60.1	0.69	88	0.23	0.38	2.9	1.4×10^5	10 mph wind, 24°C air, cloudy
8/20/69	17.6	55.0	0.71	77	0.32	0.43	3.5	1.1×10^5	12 mph wind, 20°C air, sunny
8/5/70	15.5	33	0.68	77	0.47	0.50	5.0	1.1×10^5	11 mph wind, 23°C air, sunny
9/10/71	16.3	28	0.66	68	0.58	0.75	5.3	8.3×10^4	15 mph wind, 26°C air, cloudy

Fig. 10.   Relative effluent concentration contours from the
Waukesha STP on August 5, 1970.

LEGEND

———— Concentration contours determined
from temperature data

Scale in Feet
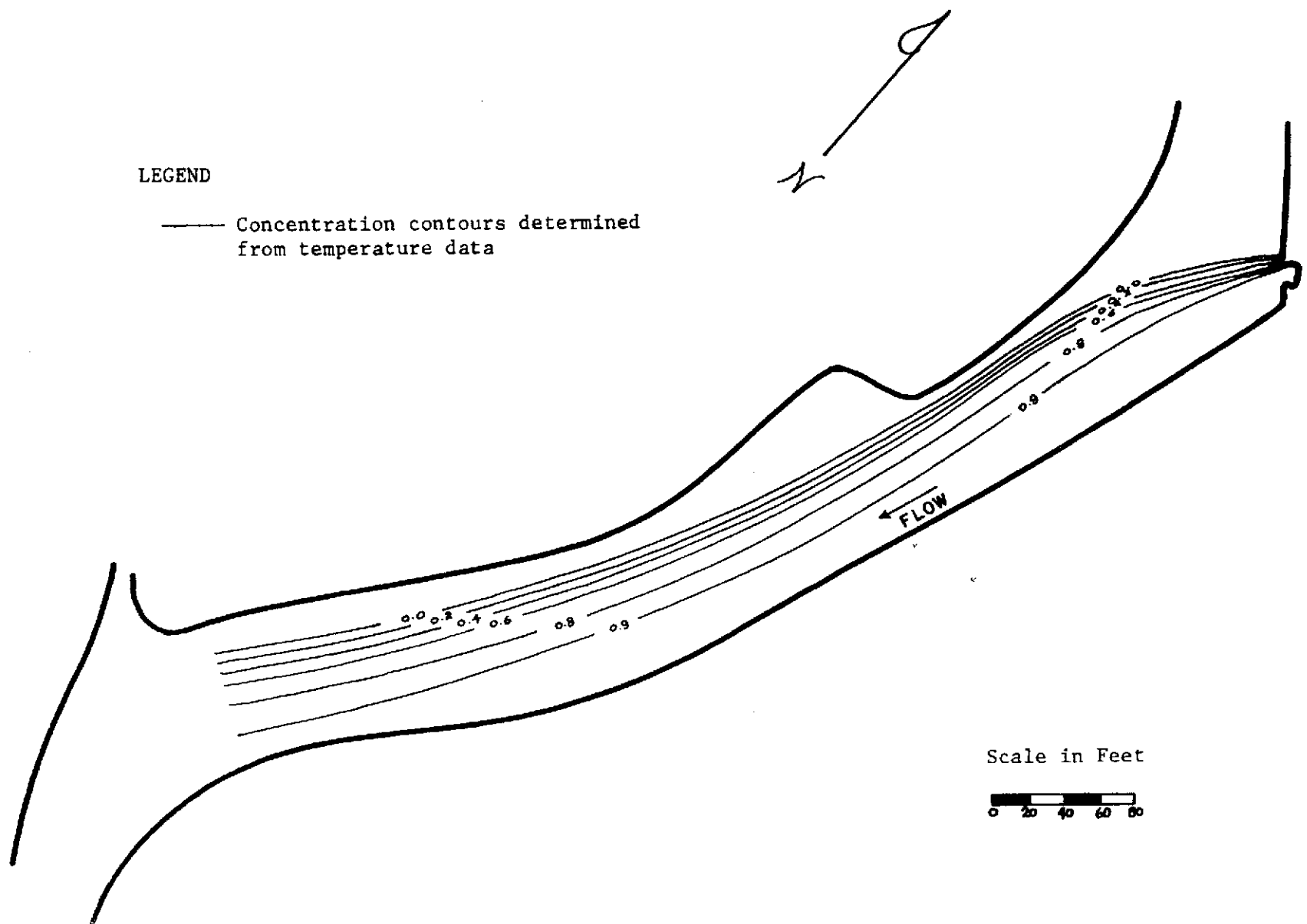
Fig. 11. Relative effluent concentration contours for
the Waukesha STP on September 10, 1971.

the physical measurements covered only 1000 to 1500 ft downstream from the outfall, it is not known if equation (6) is valid farther downstream (the river channel as noted earlier is very sinuous). However, 35 mm color photography indicates that up to 1 or 2 miles downstream the effluent discharge remains concentrated on one bank of the river, and that the effluent boundary determined photographically corresponds to half of the effluent width by ground measurements. The flow rate within the effluent boundary increases in proportion to the width, b. Initial dilution, due to entrainment, is very rapid up to 30 or 50 ft downstream of the outfall.

Estimates of the length of the mixing zone, obtained from a two-dimensional, steady-state model of the concentration distribution (including channel boundaries), are shown in Table II. Based upon these results, the mixing zone extends from 16 to 30 miles along the river and is primarily dependent upon Q_o/Q_r, that is, decreasing as Q_o/Q_r increases. Lateral mixing due to turbulent diffusion is very slow, and a lateral diffusion coefficient of $0.23 u_* d_*$ is in reasonable agreement with the measured distributions. Because the estimated lengths of the mixing zone are very long and the measurements only covered about one percent of this distance, the validity of these estimates needs to be evaluated; however, aerial photographs, as noted earlier, show that lateral mixing is very slow.

Kimberly-Clark Paper Mill. Table III summarizes river and effluent characteristics for five surveys. Figure 12 shows the effluent surface temperature distribution for one of these surveys. Figure 5, presented earlier, shows the surface temperature distribution, obtained from aerial thermal imagery, on another survey.

The effluent mixing patterns, shown in figures 5 and 12 are complex and result from various physical mechanisms. Near the plant, the 21 outfall discharges blend together and mix by entrainment of river water. Beyond 200 to 300 ft from the outfall turbulent diffusion and channel geometry and variations thereof, namely channel shape, alignment and depth, govern the mixing. Figure 13 shows the variation of effluent surface width, b, and flow rate, Q, with distance from the outfall for the survey in figure 12 and one other survey. Note that these mixing characteristics are very similar for both surveys as the effluent and river conditions are nearly the same as shown in Table III. Up to about 1500 or 2000 ft from the outfall, b and Q increase approximately as $x^{1/2}$, except for minor variations associated with the curving bank boundary, and beyond this point there is rapid lateral spreading due to a radical change in channel alignment, that is, a sharp bend and the increased depths due to the downstream dam. The temperature and suspended solids distributions downstream of this bend show the development of large scale horizontal eddy motion as well as secondary flow. Further, although the temperature and suspended solids distributions show similar trends, their distributions, as discussed below, are not similar. Although $b \sim x^{1/2}$ for $x < 1500$ to 2000 ft, the rate of

Table III. <u>Characteristics at Kimberly-Clark Paper Mill for Field Surveys</u>

Date	Q_o', cfs	Q_r', cfs	d, ft	W, ft	T_r', °C	$\Delta T_o'$, °C	Total Solids Discharged,** lb/day x 10^{-3}	$D_y/u_* d_*$	Local Climate
8/11/71	18.1	1824	8	700	24.0	15.9	40.4	--	10 mph wind, 18°C air, cloudy
8/27/71	17.9	1830	8	700	20.4	15.8	44.4	--	8.6 mph wind, 16°C air, sunny
9/16/71	16.9	1640	8	700	21.2	14.8	42.2	--	7.3 mph wind, 12°C air, cloudy
7/18/72	16.9	1781	8	700	24.2	14.8	45.5	--	6 mph wind, 21°C air, light clouds
7/19/72	15.5	1822	8	700	24.0	14.0	62.5	0.18	12 mph wind, 22°C air, sunny

** 80-85 percent mineral and 15-20 percent fibre.
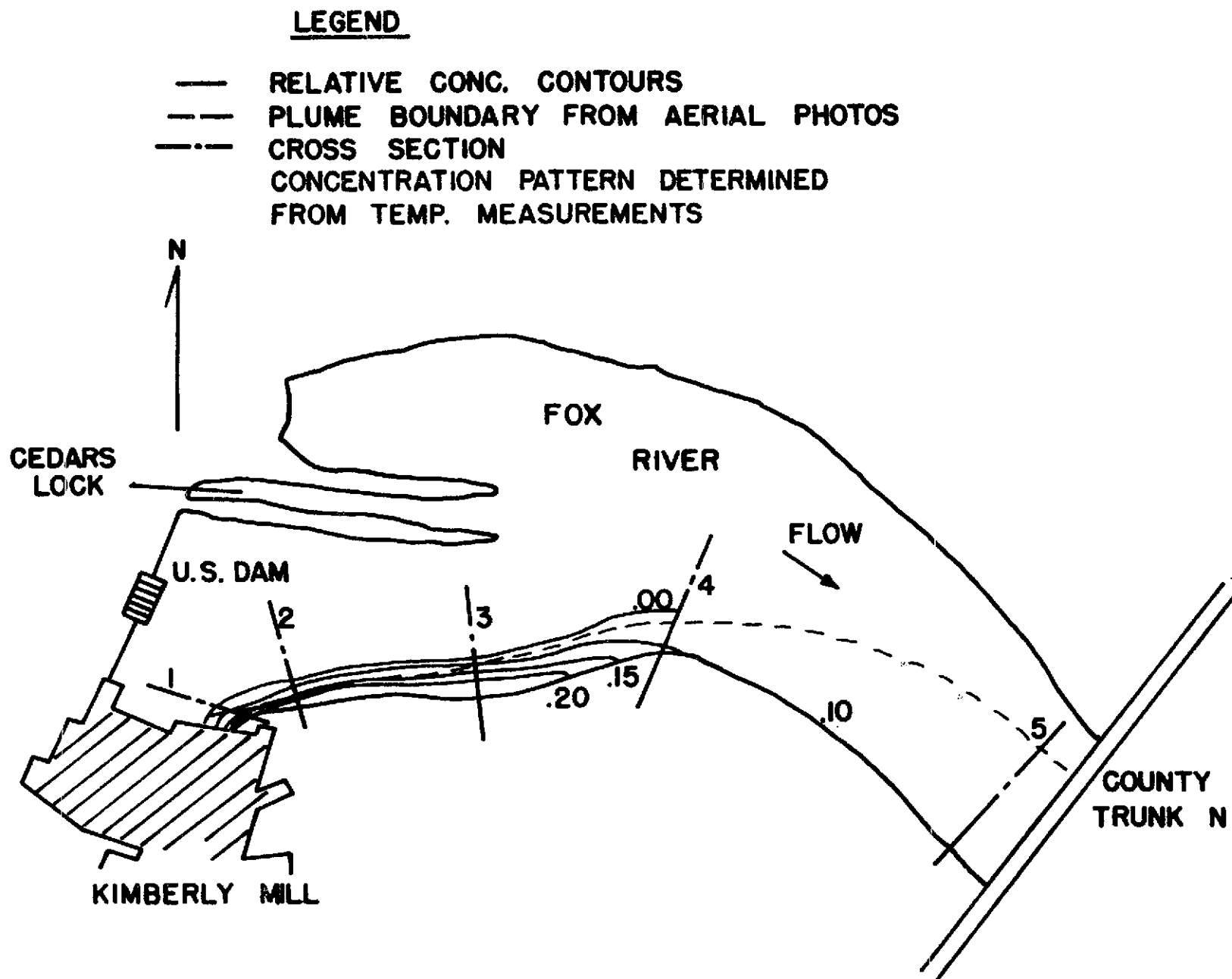
Figure 12. Relative effluent concentration contours for the Kimberly-Clark Paper Mill on August 27, 1971.

surface spread of the effluent is 2 to 4 times that due to lateral turbulent diffusion. The photographic surface boundary of the effluent for the August 27, 1971, survey (see figure 12) is in good agreement with ground measurements beyond about 1000 ft from the outfall. The discrepancy with the ground measurements close to the outfall may reflect changes in plant operations or meandering (large scale eddies) of the effluent boundary which is averaged out in the ground observations.

The vertical distributions of temperature and suspended solids up to 1000 ft from the outfall show that vertical mixing is not sufficient to produce uniform concentrations over the depth. The isotherms are inclined away from shore and there are subsurface pockets of high suspended solids concentrations. Beyond this point, vertical mixing is intense enough to produce vertical isotherms and the suspended solids show slightly greater concentrations near the bottom. As noted earlier, the distributions of temperature and suspended solids are not similar. The differences in these distributions are probably due to the weight and resultant settling of the solids, forming a sludge blanket on the bottom, and to errors of 10 ppm in the sampling of and analysis for suspended solids. Finally, the only effect noted of the meteorological conditions was an increase in the vertical mixing in response to strong winds greater than 10 to 12 mph.

No direct observations of mixing zone lengths were made as the measurements only extended to the Little Chute Dam approximately 0.75 miles downstream of the outfall. Further, estimates of mixing zone lengths based upon simple mathematical models are inadequate, because of the effects of the bend and dam. Extrapolation of the Q versus x line on figure 13 indicates that 2 to 3 miles of river are required to dilute the effluent to the average concentration of the mixing zone boundary. Suspended solids concentrations of about 10 ppm and temperatures of about $24.5^{o}C$ at the Little Chute Dam on the July 18, 1972 survey indicate that additional dilution is required. For this survey the mixing zone boundary would be given by suspended solids concentrations of 4 to 5 ppm and temperatures of $24.3^{o}C$.
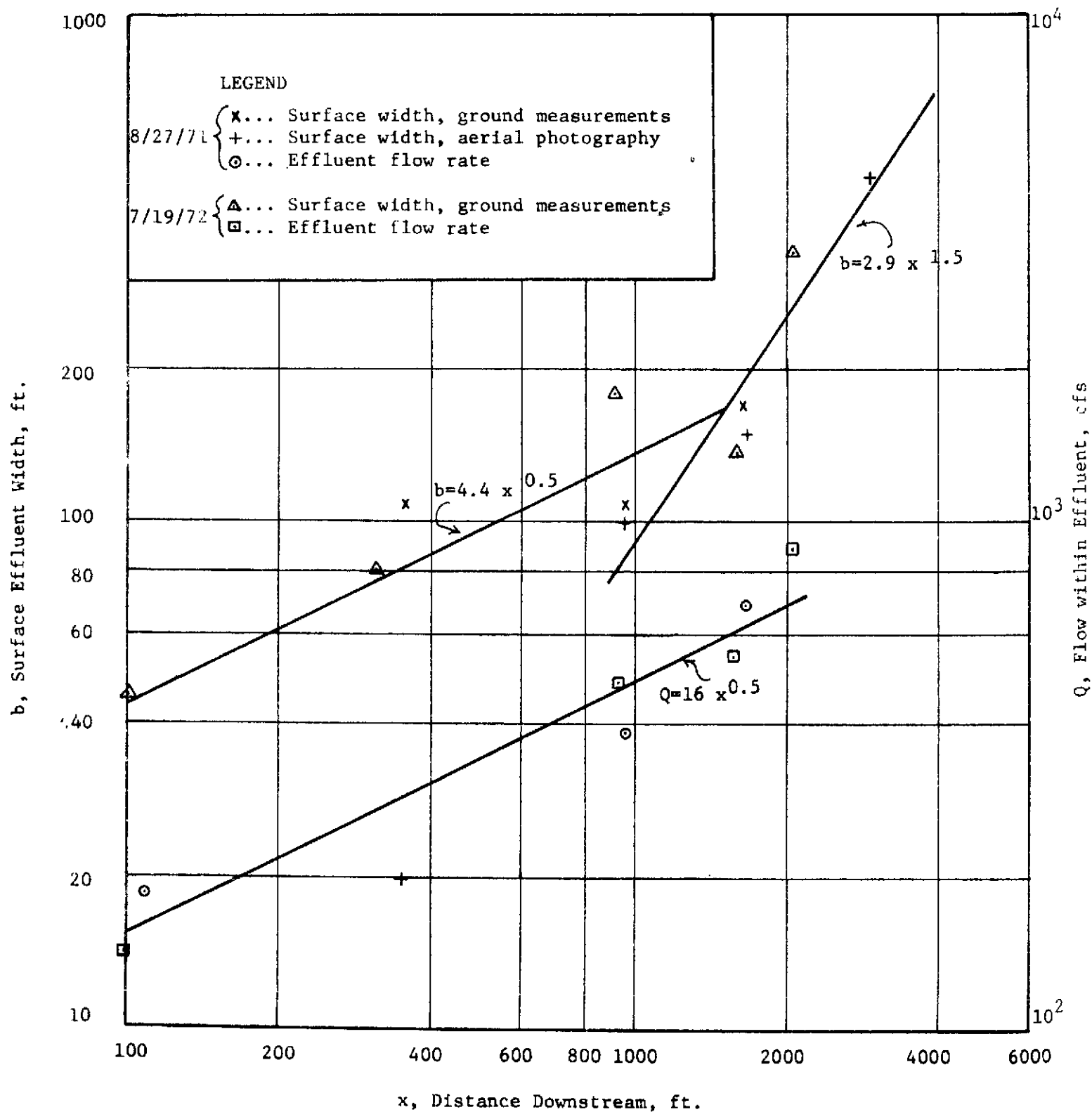
Fig. 13. Distance from outfall versus mixing zone width and discharge for the Kimberly Clark Paper Mill on August 27, 1971, and July 19, 1972.

NOMENCLATURE

A,B,C, = Parameters

B_n = Film type, handling and processing parameter ($n = 0,1,2,3$)

b = Width of mixing zone in surficial layer

b_o = Width of mixing zone in surficial layer at the end of stage one (in Eq. 6, P. 19; b_o = outfall width otherwise)

h_o = outfall depth

d = Average river depth

d_* = Local river depth

D = Image optical density

D_y = Depth averaged lateral turbulent diffusion coefficient

E = Film exposure

H_{br} = Scanner output proportional to emitted radiation

K_n = Parameter ($n = 1,2,3,4$)

L_{mz} = Estimated length of mixing zone from a 2-D Mathematic Model

Q = Total volumetric discharge rate of the mixing zone

Q_o = Effluent volumetric discharge rate at outfall

Q_r = River volumetric discharge rate just downstream from outfall

R = Water sample reflectance

S = Concentration of suspended solids

T = Temperature of the surficial layer of mixing zone

ΔT_o = Effluent temperature above that of the River at the outfall

T_r = Temperature of the ambient river

u_* = Friction velocity $(\tau_o/\rho)^{1/2}$, or $\cong 0.2\ V_r$

V_0 = Average effluent efflux velocity into river at outfall

V_r = Average river velocity for Q_r, d, and W.

W = Average river width

x = Horizontal distance from outfall

Z = Relative log E

α, β = Model parameters

ρ = Density of ambient river

ACKNOWLEDGEMENTS

REFERENCES

1. Annual Reports for the NASA Grant, Institute for Environmental Studies, University of Wisconsin-Madison, 1970-1971 and 1971-1972.

2. Dana, Robert W., "Digital Sensitometry of Color Infrared Film as an Aid To Pattern Recognition Studies", Proceedings, 2nd Annual Remote Sensing Of Earth Resources Conference, Tullahoma, Tennessee, March, 1973.

3. Holley, E. R., J. Siemons and G. Abraham, "Some Aspects of Analyzing Transverse Diffusion in Rivers", Journal Hydraulic Research, Vol. 10, No. 1, pp. 27-57, 1972.

4. Klooster, Steven A. and Scherz, James P., "Water Quality Determination By Photographic Analysis", Proceedings, 2nd Annual Remote Sensing of Earth Resources Conference, Tullahoma, Tennessee, March, 1973.

5. Prych, E. A., "Effects of Density Differences on Lateral Mixing in Open Channel Flows", Report No. KH-R-21, W. M. Keck Laboratory of Hydraulics and Water Resources, California Institute of Technology, 225 pp., May, 1970.